Sensors and Materials, Vol. 37, No. 2 (2025) 547–551
MYU Tokyo

S & M 3931

Dose Rate Response of $LaMgAl_{11}O_{19}$ Doped with Various Rare-earth Ions with NIR Luminescence

Daisuke Nakauchi,* Takumi Kato, Noriaki Kawaguchi, and Takayuki Yanagida

Nara Institute of Science and Technology (NAIST), 8916-5 Takayama, Ikoma, Nara 630-0192, Japan

(Received October 31, 2024; accepted December 16, 2024)

Keywords: scintillator, phosphor, photoluminescence, radioluminescence, afterglow

The radioluminescence and dose rate response of $LaMgAl_{11}O_{19}$ doped with rare earth single crystals were investigated. All the samples showed emission peaks at wavelengths longer than 800 nm corresponding to doped trivalent rare-earth ions. Among the prepared samples, the Nd-doped sample showed the best lower detection limit of 1.6 mGy/h, enabling highly sensitive dose measurement.

1. Introduction

Scintillators are radiation-sensitive phosphors, and single crystal,[1–4] polycrystalline,[5–8] and amorphous[9–12] forms have been investigated. Scintillators with near-infrared (NIR) luminescence have become a focal point in remote monitoring.[13–15] Remote monitoring, using a scintillator and an optical fiber, helps reduce radiation damage to signal amplifiers used for measurements.[16–19] As a monitoring system relies on optical fibers with lengths of 50–100 m, minimizing the transmission losses is critical. The transmittance of a quartz fiber from 800 to 1700 nm exceeds that in the UV–visible range,[20] and NIR light is effective in improving the transmission efficiency. In addition, since radiation-induced damage creates color centers and reduces transmittance in the visible range, NIR scintillators have an advantage. Although various rare-earth-doped scintillators were developed for applications,[21–23] to adequately monitor the inside of primary loop areas in nuclear plants during shutdown, stable measurements up to 0.1 mGy/h are required.[13]

$LaMgAl_{11}O_{19}$ is an attractive host of an NIR scintillator because $LaMgAl_{11}O_{19}$ has La^{3+} sites that are easily replaced by trivalent rare-earth ions doped as luminescent centers.[24–27] Furthermore, $LaMgAl_{11}O_{19}$ has a congruent-melting composition[28] and a lower composition ratio of rare-earth ions than conventional oxide-based scintillators such as Lu_2SiO_5 and $Gd_3Al_2Ga_3O_{12}$,[29–35] and its manufacturing cost is low because Al_2O_3 is the main component. $LaMgAl_{11}O_{19}$ has been investigated for some phosphor applications, such as lasers[36,37] and white LED technology.[38,39] However, no studies on scintillation properties for the measurement of ionizing radiation have been documented so far. In our previous work, we investigated $LaMgAl_{11}O_{19}$ doped with Nd or Er,[40,41] which have been actively studied as emission centers

*Corresponding author: e-mail: nakauchi@ms.naist.jp
https://doi.org/10.18494/SAM5425

ISSN 0914-4935 © MYU K.K.
https://myukk.org/

for laser materials. Among the investigated samples, Er-doped $LaMgAl_{11}O_{19}$ showed a detectable signal even at 1 mGy/h, which is the highest sensitivity among the NIR scintillator crystals tested so far. In this work, the dopant concentration was fixed at 1%, and several emission centers emitting in the NIR region were tested to find other promising emission centers. Radioluminescence (RL) and detector properties of various rare-earth-doped $LaMgAl_{11}O_{19}$ single crystals were investigated, and their suitability for remote monitoring applications was evaluated.

2. Data, Materials, and Methods

$RE_{0.01}La_{0.99}MgAl_{11}O_{19}$ (*RE*: Nd, Pr, Er, Tm, and Yb) crystals were synthesized using the floating zone method. First, raw powder with high purity (4N) was shaped into a cylindrical form via hydrostatic pressure and sintered at 1400 ℃ for 8 h. Then, crystal growth was conducted using a floating zone furnace (FZD0192, Canon Machinery). During crystal growth, the parameters were set at a growth speed of 5 mm/h and a rotation speed at 20 rpm. RL spectra under X-ray irradiation were measured using a spectrometer equipped with a monochromator (SR163, Andor) as well as a CCD for the UV–visible region (DU-420-BU2, Andor) and NIR region (DU492A-1.7, Andor). The X-ray generator (XRB80N100/CB, Spellman) was used as an excitation source with a bias voltage of 80 kV and a tube current of 1.2 mA. Dose rate responses were measured using the original system composed of an optical fiber (600 µmφ × 5 m) and an InGaAs PIN photodiode (G12180-250A, Hamamatsu Photonics).[21]

3. Results and Discussion

The prepared samples were crushed to appropriate sizes, and then one large surface was polished to conduct the following measurements. The photographs of the $LaMgAl_{11}O_{19}$:*RE* samples are shown in Fig. 1, and all the samples appear colorless and transparent and contain a few cracks.

Figure 2 shows the RL spectra obtained upon X-ray exposure in the UV–visible (180–700 nm) and NIR (700–1624 nm) regions. In the UV–visible region, all the samples exhibit a broad

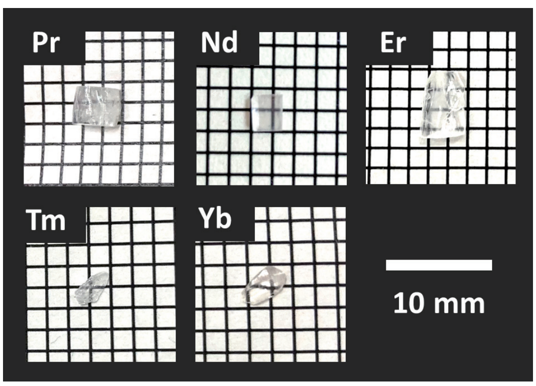

Fig. 1. (Color online) Photographs of $LaMgAl_{11}O_{19}$:*RE*.

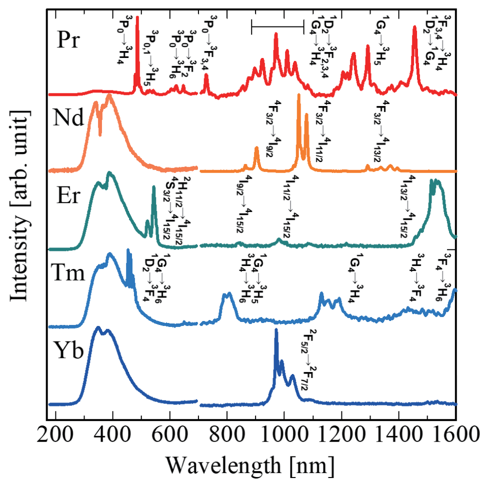

Fig. 2. (Color online) RL spectra of $LaMgAl_{11}O_{19}$:*RE*.

emission peak at 300–500 nm, which was also observed in previously reported $LaMgAl_{11}O_{19}$ doped with Ce or Nd.[40,42] Therefore, the emission origin is intrinsic luminescence. In the Nd- or Er-doped samples, a sharp valley at 380 nm changes the shape of the host emission band owing to the absorption of Nd^{3+} [$^4I_{9/2}$–$^4D_{5/2}$, $^4D_{3/2}$, $^4D_{1/2}$,[43]] or Er^{3+} [$^4I_{15/2}$–$^4G_{11/2}$,$^4G_{9/2}$[44,45]]. In the NIR range, several sharp emission peaks are observed at the wavelength suitable for the sensitivity of the Si photodiode.

Figure 3 illustrates the correlation between the X-ray irradiation dose rate and the output signal. The measured signals were approximated using power functions ($y = ax^b$). In the analyses, using the 3σ method (σ: standard deviation), the lower detection limit was determined by comparing 3σ values based on the signal without irradiation. The 3σ values for Nd and other ions differ depending on the measurement date. The measurement limits determined by the 3σ method are summarized in Table 1. The detection limit values of all the samples were lower than 10 mGy/h, with the Nd-doped sample showing the best lower detection limit of 1.6 mGy/h. However, the Nd-doped sample shows the lowest proportionality (sublinearity), which may be due to the trap level related to the afterglow or ionization quenching occurring under high dose rates, but the current results do not reveal why this is only seen in the Nd-doped sample. They notably exceed the detection limit of conventional methods utilizing UV–visible scintillators, such as Gd_2O_2S:Pr combined with Si photodiodes (800 mGy/h).[13] Furthermore, these results are comparable to the best performance previously achieved in our studies using the same measurement system: $GdVO_4$:Nd (6 mGy/h [21]) and $Bi_4Ge_3O_{12}$:Er (6 mGy/h[45]).

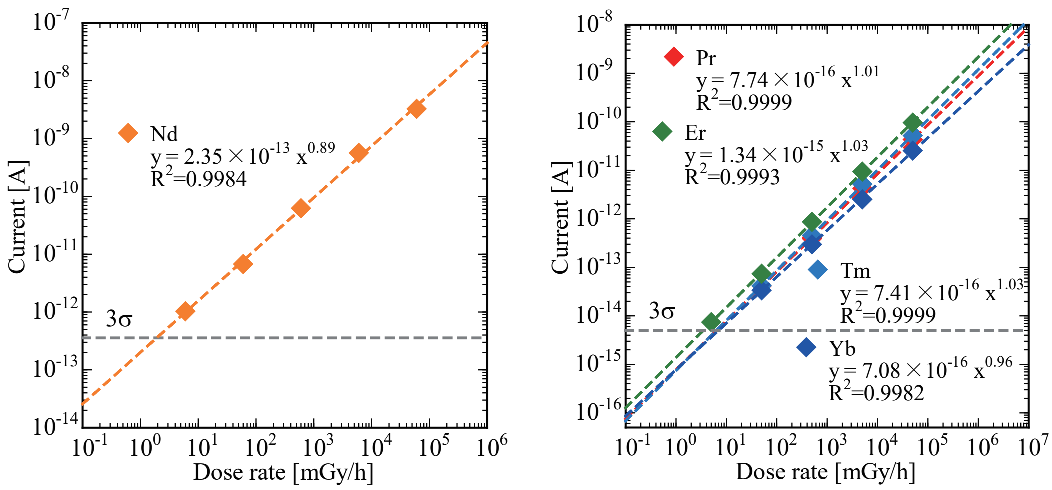

Fig. 3. (Color online) Dose rate response of $LaMgAl_{11}O_{19}$:*RE*.

Table 1
Lower detection limits of $LaMgAl_{11}O_{19}$:*RE* and reported crystal scintillators.

Sample	Detection limit (mGy/h)	Sample	Detection limit (mGy/h)
$LaMgAl_{11}O_{19}$:Nd	1.6	$GdVO_4$:Nd	6.0[21]
$LaMgAl_{11}O_{19}$:Pr	6.1	$Bi_4Ge_3O_{12}$:Er	6.0[45]
$LaMgAl_{11}O_{19}$:Er	4.8/1.0[41]	$Bi_4Ge_3O_{12}$:Nd	10[22]
$LaMgAl_{11}O_{19}$:Tm	6.7	$Bi_4Ge_3O_{12}$:Tm	30[46]
$LaMgAl_{11}O_{19}$:Yb	7.7	CsI:Nd	60[47]

4. Conclusions

Rare-earth-doped $LaMgAl_{11}O_{19}$ single crystals were synthesized to comprehensively investigate the RL and dose rate responses. Upon X-ray irradiation, several sharp emission peaks attributed to the 4f–4f transition of trivalent rare-earth ions were observed in the NIR region suitable for the target wavelength sensitive to the InGaAs detector. When investigating the correlation between the X-ray exposure dose rate and the output signal, all tested samples showed good linearity over a wide dynamic range. The Nd-doped sample exhibited the best lower detection limit of 1.6 mGy/h. This surpassed those of other NIR crystal scintillators reported previously. Consequently, Nd-doped $LaMgAl_{11}O_{19}$ stands out as a promising candidate for use in scintillation detectors designed for remote monitoring applications.

Acknowledgments

This work was supported by JSPS KAKENHI (22H00309, 23K21827, 23K25126, 24K03197, 22K18997, and 23K13689), Suzuki Foundation, and Asahi Glass Foundation.

References

1 D. Shiratori, H. Fukushima, D. Nakauchi, T. Kato, N. Kawaguchi, and T. Yanagida: Sens. Mater. **35** (2023) 439.
2 H. Fukushima, D. Nakauchi, T. Kato, N. Kawaguchi, and T. Yanagida: Sens. Mater. **35** (2023) 429.
3 T. Yanagida, K. Watanabe, T. Kato, D. Nakauchi, and N. Kawaguchi: Sens. Mater. **35** (2023) 423.
4 K. Miyazaki, D. Nakauchi, T. Kato, N. Kawaguchi, and T. Yanagida: Sens. Mater. **36** (2024) 515.
5 D. Nakauchi, F. Nakamura, T. Kato, N. Kawaguchi, and T. Yanagida: Sens. Mater. **35** (2023) 467.
6 M. Koshimizu, Y. Fujimoto, and K. Asai: Sens. Mater. **35** (2023) 521.
7 T. Kunikata, T. Kato, D. Shiratori, P. Kantuptim, D. Nakauchi, N. Kawaguchi, and T. Yanagida: Sens. Mater. **35** (2023) 491.
8 T. Kato, D. Nakauchi, N. Kawaguchi, and T. Yanagida: Sens. Mater. **36** (2024) 531.
9 N. Kawaguchi, K. Watanabe, D. Shiratori, T. Kato, D. Nakauchi, and T. Yanagida: Sens. Mater. **35** (2023) 499.
10 Y. Takebuchi, D. Shiratori, T. Kato, D. Nakauchi, N. Kawaguchi, and T. Yanagida: Sens. Mater. **35** (2023) 507.
11 Y. Oshima, K. Watanabe, H. Shiga, and G. Wakabayashi: Sens. Mater. **35** (2023) 545.
12 D. Nakauchi, H. Kimura, D. Shiratori, T. Kato, N. Kawaguchi, and T. Yanagida: Sens. Mater. **36** (2024) 573.
13 E. Takada, A. Kimura, Y. Hosono, H. Takahashi, and M. Nakazawa: J. Nucl. Sci. Technol. **36** (1999) 641.
14 E. Takada: IEEE Trans. Nucl. Sci. **45** (1998) 556.
15 A. Kimura, E. Takada, Y. Hosono, M. Nakazawa, H. Takahashi, and H. Hayami: J. Nucl. Sci. Technol. **39** (2002) 603.
16 A. L. Huston, B. L. Justus, P. L. Falkenstein, R. W. Miller, H. Ning, and R. Altemus: Nucl. Instrum. Methods Phys. Res. B **184** (2001) 55.
17 S. O'Keeffe, D. McCarthy, P. Woulfe, M. W. D. Grattan, A. R. Hounsell, D. Sporea, L. Mihai, I. Vata, G. Leen, and E. Lewis: Br. J. Radiol. **88** (2015) 20140702.
18 G. Bartesaghi, V. Conti, M. Prest, V. Mascagna, S. Scazzi, P. Cappelletti, M. Frigerio, S. Gelosa, A. Monti, A. Ostinelli, A. Mozzanica, R. Bevilacqua, G. Giannini, P. Totaro, and E. Vallazza: Nucl. Instrum. Methods Phys. Res. A **572** (2007) 228.
19 M. Ishikawa, K. Ono, Y. Sakurai, H. Unesaki, A. Uritani, G. Bengua, T. Kobayashi, K. Tanaka, and T. Kosako: Appl. Radiat. Isot. **61** (2004) 775.
20 M. Ding: Handbook of Optical Fibers, (Springer, 2018), Part V Special Optical Fibers.
21 M. Akatsuka, H. Kimura, D. Onoda, D. Shiratori, D. Nakauchi, T. Kato, N. Kawaguchi, and T. Yanagida: Sens. Mater. **33** (2021) 2243.
22 K. Okazaki, D. Onoda, H. Fukushima, D. Nakauchi, T. Kato, N. Kawaguchi, and T. Yanagida: J. Mater. Sci. Mater. Electron. **32** (2021) 21677.
23 D. Nakauchi, G. Okada, M. Koshimizu, and T. Yanagida: J. Rare Earths **34** (2016) 757.

24 J. M. P. J. Verstegen, J. L. Sommerdijk, and J. G. Verriet: J. Lumin. **6** (1973) 425.
25 V. Singh, R. P. S. Chakradhar, J. L. Rao, and H. Y. Kwak: J. Lumin. **131** (2011) 247.
26 J. L. Sommerdijk, J. A. W. van der Does de Bye, and P. H. J. M. Verberne: J. Lumin. **14** (1976) 91.
27 X. Luo, X. Yang, and S. Xiao: Mater. Res. Bull. **101** (2018) 73.
28 S. C. Abrahams, P. Marsh, and C. D. Brandle: J. Chem. Phys. **86** (1987) 4221.
29 C. M. Pepin, C. St-Pierre, J.-C. Forgues, Y. Kurata, N. Shimura, T. Usui, T. Takeyama, H. Ishibashi, and R. Lecomte: IEEE Nucl. Sci. Symp. Conf. Rec. (2007) 2292.
30 I. Gerasymov, O. Sidletskiy, S. Neicheva, B. Grinyov, V. Baumer, E. Galenin, K. Katrunov, S. Tkachenko, O. Voloshina, and A. Zhukov: J. Cryst. Growth **318** (2011) 805.
31 M. Tanaka, K. Hara, S. Kim, K. Kondo, H. Takano, M. Kobayashi, H. Ishibashi, K. Kurashige, K. Susa, and M. Ishii: Nucl. Instrum. Methods Phys. Res. A **404** (1998) 283.
32 W. W. Moses, S. E. Derenzo, A. Fyodorov, M. Korzhik, A. Gektin, B. Minkov, and V. Aslanov: IEEE Trans. Nucl. Sci. **42** (1995) 275.
33 M. Moszyński, D. Wolski, T. Ludziejewski, M. Kapusta, A. Lempicki, C. Brecher, D. Wiśniewski, and A. J. Wojtowicz: Nucl. Instrum. Methods Phys. Res. A **385** (1997) 123.
34 C. W. E. van Eijk, J. Andriessen, P. Dorenbos, and R. Visser: Nucl. Instrum. Methods Phys. Res. A **348** (1994) 546.
35 T. Yanagida, K. Kamada, Y. Fujimoto, H. Yagi, and T. Yanagitani: Opt. Mater. **35** (2013) 2480.
36 Z. Y. Gao, G. Q. Xia, X. Yan, J. F. Zhu, X. D. Xu, and Z. M. Wu: Opt. Rev. **28** (2021) 404.
37 J. Wang, Y. Zhang, X. Guan, B. Xu, H. Xu, Z. Cai, Y. Pan, J. Liu, X. Xu, and J. Xu: Opt. Mater. **86** (2018) 512.
38 W. Li, G. Fang, Y. Wang, Z. You, J. Li, Z. Zhu, C. Tu, Y. Xu, and W. Jie: Vacuum **188** (2021) 110215.
39 X. Min, Z. Huang, M. Fang, Y. Liu, C. Tang, and X. Wu: Inorg. Chem. **53** (2014) 6060.
40 D. Nakauchi, T. Kato, N. Kawaguchi, and T. Yanagida: Sensors **22** (2022) 9818.
41 D. Nakauchi, T. Kato, N. Kawaguchi, and T. Yanagida: Radiat. Meas. **175** (2024) 107174.
42 L. Nádherný, V. Doležal, D. Sedmidubský, J. Cajzl, R. Kučerková, M. Nikl, V. Jakeš, and K. Rubešová: J. Mater. Res. **35** (2020) 1672.
43 E. Ceci-Ginistrelli, C. Smith, D. Pugliese, J. Lousteau, N. G. Boetti, W. A. Clarkson, F. Poletti, and D. Milanese: J. Alloys Compd. **722** (2017) 599.
44 P. Babu, H. J. Seo, K. H. Jang, R. Balakrishnaiah, C. K. Jayasankar, K.-S. Lim, and V. Lavín: J. Opt. Soc. Am. B **24** (2007) 2218.
45 K. Okazaki, H. Fukushima, D. Nakauchi, G. Okada, D. Onoda, T. Kato, N. Kawaguchi, and T. Yanagida: J. Alloys Compd. **903** (2022) 163834.
46 K. Okazaki, D. Nakauchi, H. Fukushima, T. Kato, N. Kawaguchi, and T. Yanagida: Sens. Mater. **35** (2023) 459.
47 S. Takase, K. Miyazaki, D. Nakauchi, T. Kato, N. Kawaguchi, and T. Yanagida: J. Lumin. **267** (2024) 120400.